Journal of Rehabilitation in Civil Engineering 6-2 (2018) 115-138

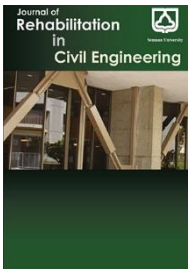

journal homepage: http://civiljournal.semnan.ac.ir/

Impact of Loading Protocol on the Performance of the Steel Moment Frame Connections

M. Ghassemieh[1*] and A. Rahimzadeh[2]
1. School of Civil Engineering, University of Tehran
2. MS Graduate Student, University of Tehran

Corresponding author: *m.ghassemieh@ut.ac.ir*

ARTICLE INFO

Article history:
Received 18 April 2017
Accepted: 31 October 2017

Keywords:
Loading Protocol,
Moment Connection,
Finite Element,
Cyclic Behavior,
Ductility.

ABSTRACT

Today, for the moment frame structures, seismic provisions of the structural engineering design codes depend on the inelastic deformation as well as inelastic capacity of the connections. A cyclic loading protocol is normally exercised for measuring such capability. This paper investigates the deformation capacity of steel moment resisting frame's connections subjected to different loading protocols. To evaluate the performance of the connections subjected to various cyclic loads, behavior of three types of connections is studied. Behavior and capacity of each connection are assessed subjected to different loading protocols; namely ATC, FEMA and SAC. The results from this research indicate that the ATC and FEMA loading make greater demands on the connections; while SAC basic loading shows a better agreement with the target values of the loading protocol. A loading protocol has been developed taking some criteria into account in order to match the target values presented in SAC study for steel moment connection's bam to column sub-assemblies. Then the connections were subjected once again to the proposed loading protocol and results compared to those of other loading protocols. The results reveal that the connections subjected to the proposed loading protocol provide greater deformation and strength capacity. Also, lower equivalent plastic strain and lower dissipated energy were observed when the connection is subjected to the proposed loading protocol.

1. Introduction

Due to the stochastic nature of ground motions, every ground motion has its unique characteristics in terms of magnitude, intensity, duration, and frequency content. As a result, there is a high degree of uncertainty in the earthquake damage prediction. For

DOI: 10.22075/JRCE.2017.11088.1182

dramatic consequences of the damages caused by earthquakes on structures, development of improved loading protocols for testing structural components against potential seismic loads is essential.

Extensive damages on beam-to-column connections of steel structures that they experienced in the Northridge earthquake emphasized the need to modify the existed design procedure for these types of connections. In order to evaluate the deformation capacities of the existing and new connection details, loading histories that represent a vast domain of possible forces caused by a seismic excitation is necessary. These loading histories are used to match the deformation demands of connections in an earthquake event as closely as possible.

Various loading protocols are developed for steel moment resisting frames' connections such as ATC-24 [1], the loading protocol developed for steel structures and components [2], loading protocol for beam to column subassemblies [3], FEMA 461 loading protocol for structural and nonstructural components [4]. Many other loading protocols have been developed for different types of structural and non-structural components such as Crescendo protocol [5], the loading protocol developed for testing wood frame structures [6], EN-12512 protocol [7], SUNY-Buffalo NCS protocol [8] and the protocol for nonstructural window systems [9]. Different countries have their unique approaches and loading protocols for their evaluation procedures, however some of the studies on loading protocols had greater impacts and novelty which some of them are discussed below in order for reader to get familiar with latest work on the topic.

Yu et al. [10] investigated the effect of load sequence on cyclic performance of RBS connections. This study revealed the appropriate seismic performance for this connection. No weld failure was observed prior to the 0.03 rad this study target plastic rotation. Moreover, the specimen loaded by the near-fault loading protocol reached a plastic rotation capacity twice the capacity reached by the standard loading protocol. No low-cycle fatigue failure in flanges of the specimen tested with near-fault loading protocol [2] were observed. It was found that energy dissipation capacity of the reduced beam section of the connection is not dependent on the type of loading history. The specimen tested by the near-fault loading history experienced buckling prior to the specimen tested by the standard loading protocol at the same drift level.

In a study Gatto and Uang [11] investigated the effects of loading protocol on the response of wood frame with shear wall. They compared ISO [12], Porter [13] and the latest loading protocols of the CUREE study [6] in addition to a monotonic loading in their study. Gatto and Uang [11] had two types of test specimen. They evaluated performance, failure mode, strength, stiffness, deformation capacity and absorbed energy of shear walls. The loading protocol of the CUREE study resulted in failure modes that coincided with seismic behavior of the structures. Consequently, Gatto and Uang [11] made a suggestion to use this protocol as a standard protocol for future tests of wooden frames.

Okazaki et al. [14] tested six specimens of link beams in eccentrically braced frames by applying them AISC loading protocol [15] which was developed by Richards and Uang [16]. They developed a loading protocol for

short links in eccentrically braced frames. The specimens subjected to the loading protocol showed a rotation capacities 50% higher than the ones tested by the AISC loading protocol. Moreover, studied links showed design rotation capacities higher compared to the assumed values.

All the aforementioned was studies conducted for structural element; in contrast, Shafei and Zareian [17] developed a loading protocol for displacement-sensitive nonstructural components. Based on the analytical and experimental studies and observations of damage in the past earthquakes, they concluded that loading histories have considerable effect on nonstructural damage, and choosing the appropriate loading protocol is important to evaluate the performance of these components.

Jiao et al. [18] investigated beams' behavior under loading protocols and compared them with analytical beam responses. The appropriate combinations of the loading protocols employed in beam tests for the purpose of evaluating the seismic behavior of steel beams were suggested. This study focused on the investigation of loading protocols employed in beam testing. Beam seismic performance in a weak-beam moment frame under various earthquakes has been obtained through response analysis and in-plane beam analysis. By comparing the beams performance under the recommended Japanese and American loading protocols and that under ground-motions, suggestions were made by Jiao et al. [18] on the selection of loading protocols in beam tests for the purpose of evaluating the seismic performance of the beam. Those suggestions for single specimen and multiple specimen testing program are detailed below.

Single specimen testing program:
One loading protocol from the SAC 2000/ASIC, FEMA 461, or JISF loading protocols.

Multiple specimens testing program:
Testing program with at least three specimens is recommended.

1) One loading protocol from the SAC/ASIC, FEMA 461, or JISF loading protocol.
2) One constant amplitude with small loading amplitude, for example: ± 38P.
3) Either the monotonic loading or the SAC-Near-fault loading protocol.

In an analysis performed by Bazaez and Dusicka [19], numerous subduction ground motions were imposed on structures with a wide range of structural periods, and a representative numerical model of the hysteretic behavior of ductile reinforced concrete columns was utilized. Since the number of inelastic cycles and the overall damage are closely related, statistical analyses of the number of inelastic cycles and cumulative inelastic demands were employed. Due to the dependence of these parameters on the structural period, different protocols were developed for short, medium and long period response. The proposed cyclic deformation histories are more representative of inelastic demands from subduction mega earthquakes and therefore their application would improve the seismic assessment of bridge columns through testing.

In another study, Megros and Beyer [20] developed a cyclic loading protocols for European regions of low to moderate seismicity. In this study, cumulative damage demands imposed by a set of 60 ground motion records were evaluated for a wide

variety of SDOF systems that reflected the fundamental properties of a large portion of the existed building stock. The ground motions were representative of the seismic hazard level corresponding to a 2% probability of exceedance in 50 years in a European moderate seismicity region. To meet the calculated cumulative damage demands, loading protocols for different structural types and vibration periods were developed.

In Fig. 1 Megros and Beyer [20] compared the cumulative demand parameters of the median normalized cycle amplitude sequences as derived from the 60 low to moderate seismicity ground motion records with those from the 20 high seismicity records [6]. The figure clearly underscores that high seismicity records impose higher cumulative demands than low to moderate seismicity records. This applies in particular to the elastic systems or systems responding in the low ductility range, which are also the systems subjected to the largest cumulative demands and which will therefore govern the design of loading protocols. This finding by Megros and Beyer [20] supports the usage of different loading protocols for low to moderate seismicity regions and high seismicity regions. It is recalled that Fig. 1 refers to the sum of normalized cycle amplitudes with respect to the maximum displacement Δmax.

As it is shown in Fig. 2 Megros and Beyer [20] found that $\Sigma\delta i$ (sum of normalized cycle amplitudes) tends to decrease as the period of vibration increases. As a result, the $\Sigma\delta i$ demands for periods equal to or longer than 0.5s are significantly smaller than the $\Sigma\delta i$ demands for periods between 0.1s and 0.3s.

When Megros and Beyer [20] new protocols compared to the existed ones [4, 6, 22], the new protocols for regions of low to moderate seismicity were, as expected, significantly less demanding than the existing loading protocols. Hence, the application of the Megros and Beyer protocols for low to moderate seismicity may lead to less conservative estimations of structural capacities. The CUREE [6] and FEMA-461 [4] loading protocols impose similar cumulative demands than the new protocols for high seismicity if the period of vibration is less than 0.5s. CUREE and FEMA- 461 have been found less demanding for stiff elastic systems (T=0.1s) in high seismicity regions and more demanding for all flag-shaped hysteretic systems.

In another study performed by Megros and Beyer [21] new loading protocols have been developed for structures designed for different behavior factors. The new loading protocols expected to yield more realistic estimates of structural strength and deformation capacities when applied to test specimens since they represent more accurately anticipated cumulative damage demands. Previous loading protocols have been developed independently of the value of the behavior factor that the structure has been designed for. Conservatively, a single loading protocol has been adopted by Megros and Beyer [21], for all behavior factor values, based on the structural system with the most difficult cumulative seismic demands. However, analyses conducted by the authors, showed that imposed cumulative seismic demands decrease significantly for structures designed for high behavior factors. The conclusion has been made by the authors that adopting a single loading protocol for the most demanding behavior factor value may lead to the derivation of highly conservative

loading protocols for the rest of the structural systems.

In this study, the impact of loading protocols on the behavior of steel moment resisting frame's connections is investigated in different aspects. First, the demand exerted on the connection by each loading protocols is evaluated.

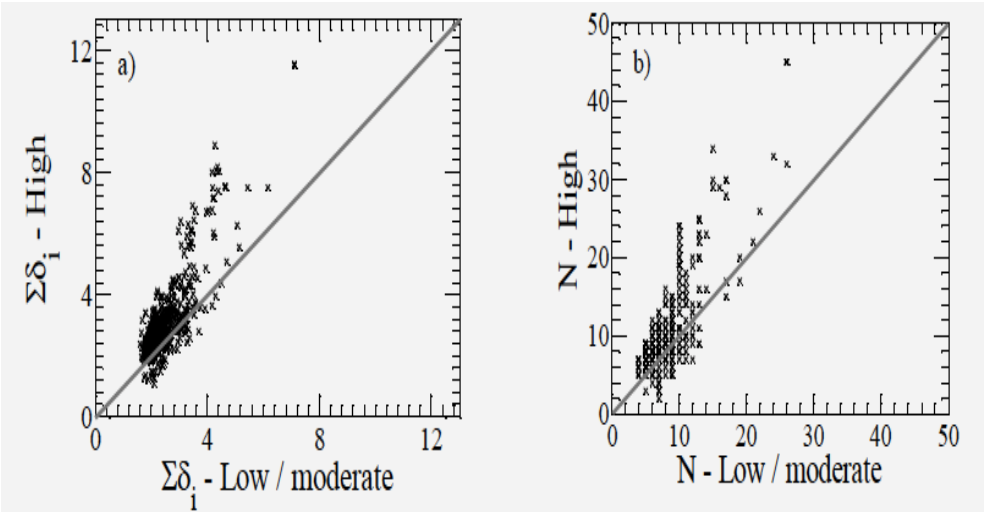

Fig. 1. Comparison of cumulative seismic demand parameters calculated for low to moderate and high seismicity regions [20].

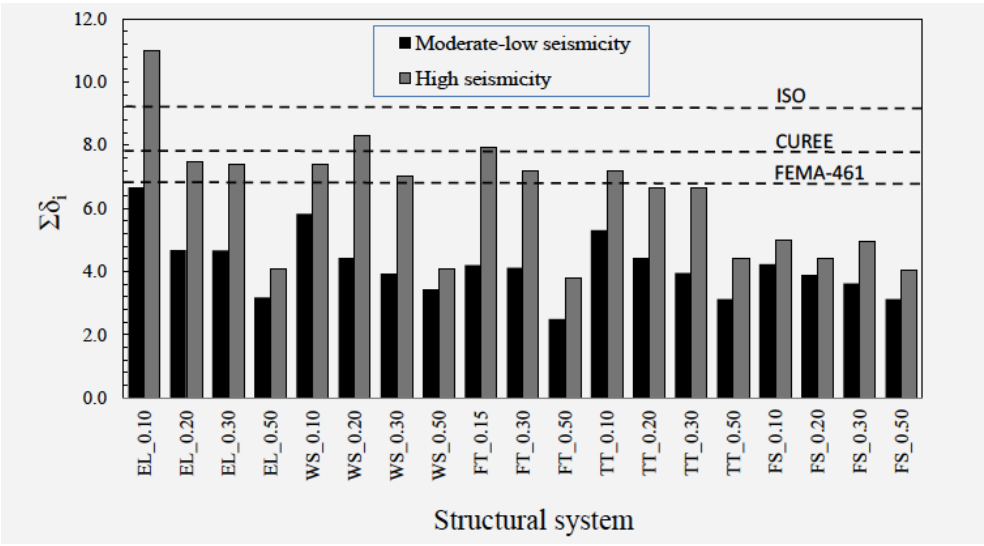

Fig. 2. Comparison of proposed and existing loading protocols in terms of Σδi [20].

Then, behavior of the connection subjected to the loading histories, and parameters such as deformation and strength capacity, equivalent plastic strain and dissipated energy of each connection subjected to various loading sequence are evaluated. In addition, failure mode of the connections is examined. Each connection compared to its equivalent in order to perceive a complete understanding of connection in different loading situations. Finally, a new loading protocol, which matches the demands parameters imposed on the connections and alleviates the shortcomings of the existing loading protocols, is proposed. Then, proposed

loading applied to three connection types with the intention of further investigation.

2. Connections Case Study

The beam-to-column connections used in this study are chosen from flange plate connections designed in accordance with AISC [23-24]. Table 1 shows general information about the buildings for which these connections are designed. Connections, which are used in this study, categorized in as light, medium and heavy size connections; representing wide range of the connection sizes. The detailing and dimensions of the medium size connection is illustrated in Fig. 3. As it shown in Fig. 4, in the experimental program, all connection subassemblies are T-shaped, and include one-half of the beam length and a whole column length. In each connection subassembly, the two ends of the column are pinned, while, a moment hinge is placed in the beam end located at the mid-span of the beam [25-26]. Further details are provided in the following references [23-24].

Table 1. Designed frame

No. of Stories	No. of Spans x-dir.	No. of Spans y- dir.	Span length (m)	Story height (m)
7	5	5	5	3
12	5	5	5	3
20	5	5	5	3

3. The Loading History

All connections are loaded by ATC-24, SAC basic and SAC near-fault [2], FEMA-461 [4] loading histories, as well as a monotonic loading. These loading histories are shown in Fig. 5. In the SAC basic loading history, the control parameter is inter-story drift angle. The ATC-24 loading protocol uses the story yielding drift as a coefficient to determine the amplitudes of the loading cycles. In the FEMA-461 loading history, each loading step consists of two cycles with constant amplitude. Meanwhile, Δ_m is the maximum target deformation amplitude of the loading history, and is the amount of the imposed deformation that is expected to cause minimum damage. Δ_m is determined by a monotonic test, before the cyclic test.

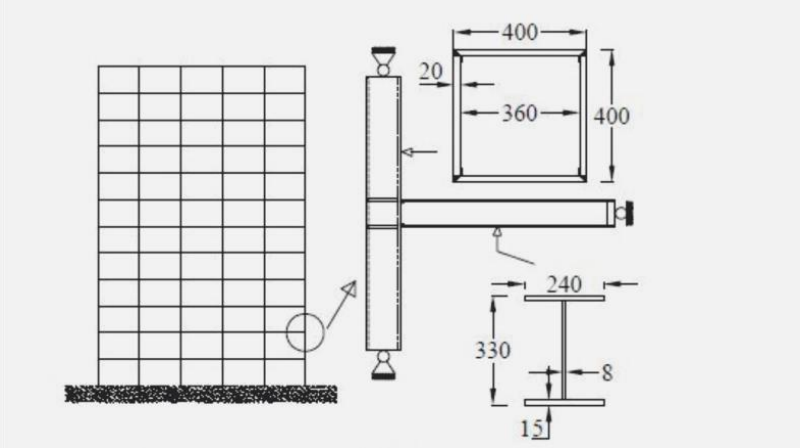

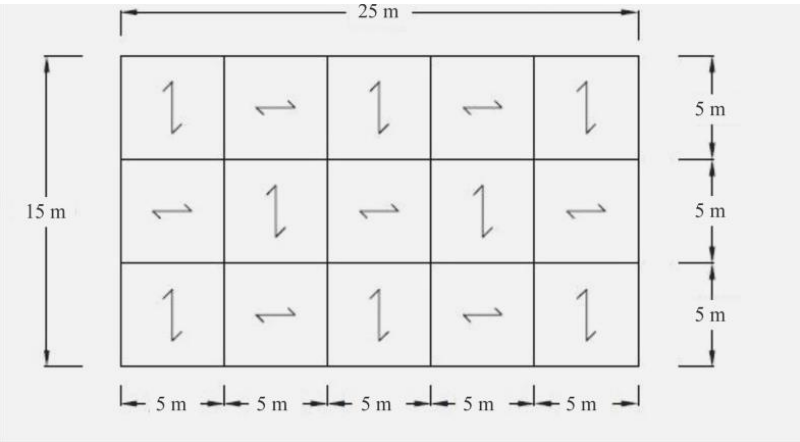

Fig. 3. The exterior connection with column and beam section [23-24].

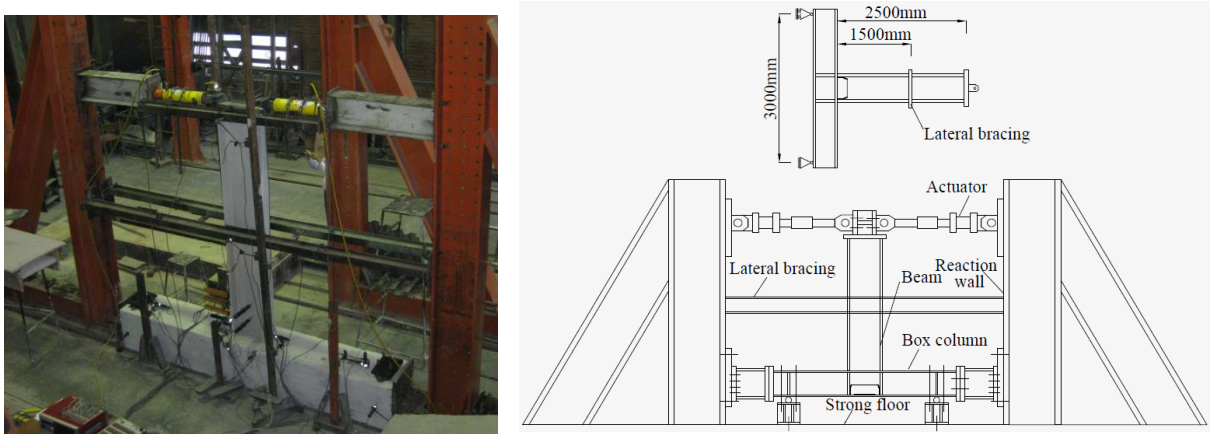

Fig. 4. Test set up for the experimental program [23-24].

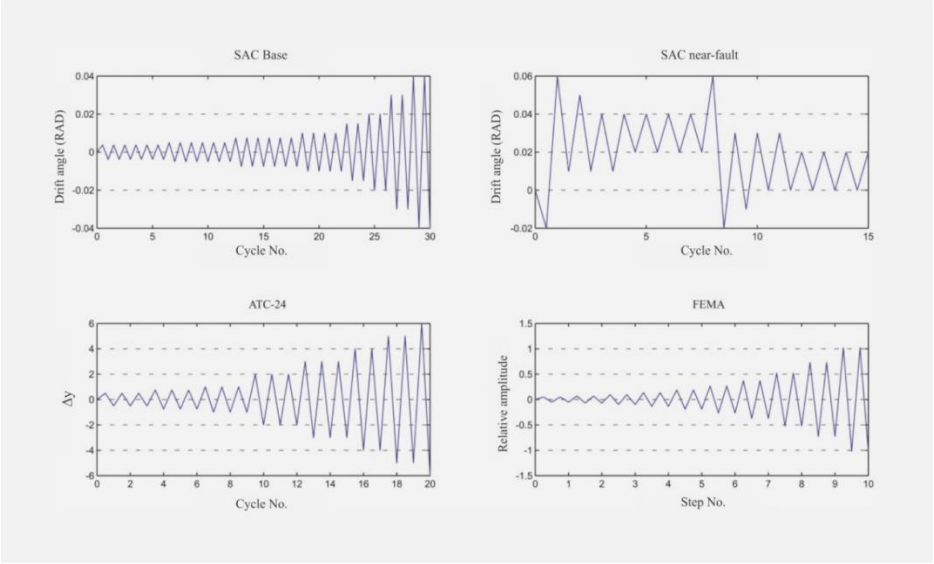

Fig. 5. Cyclic loading protocols used in this study.

4. Finite Element Modeling of the Connection

All connections are modeled and then analyzed by ABAQUS Finite Element computer software [27]. Reduced integration was used because of the high stress concentration in the connection region. Thus, the 20-node quadratic brick element (C3D20R) is used for this purpose. However, in the regions of the connection subassembly where there is a lower amount of stress concentration, eight node linear brick elements (C3D8R0) are used. In Fig. 6, the final converged finite element mesh of the medium sized connection is presented.

The results obtained from the finite element analysis are compared with the behavior of the corresponding test specimens loaded by the SAC basic loading history. Using the bilinear behavior of ST-37 steel, the stress-strain material behavior in finite element model is selected based on the coupon test results. As demonstrated in Fig. 7, all finite element connection models validated by comparing the moment rotation behavior of the connections in test specimen and their equivalent FE model. As shown in Fig. 7, the behavior of the finite element model is quite close to the behavior of the test specimen. After validating the finite element model and ensuring the accuracy of the FE modeling, the models are loaded by monotonic and cyclic loads.

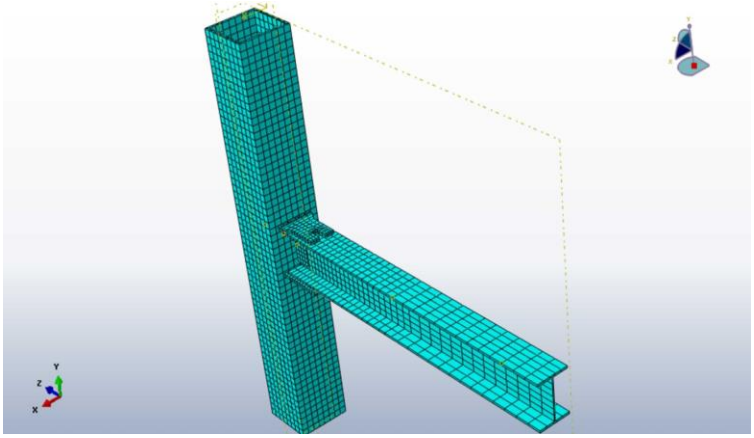

Fig. 6. Finite Element model of the connection

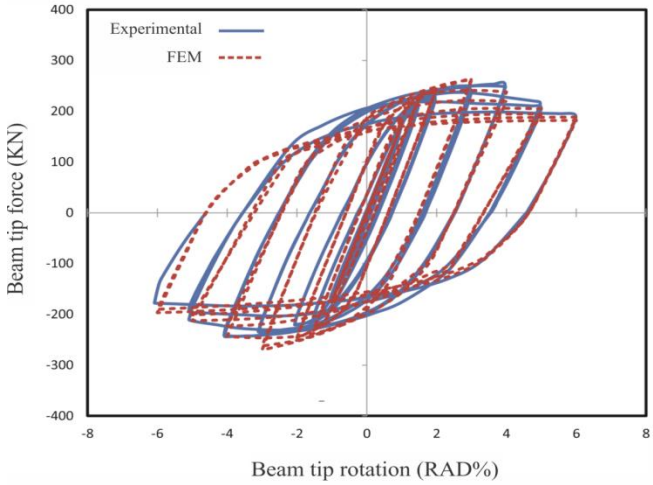

Fig. 7. Hysteresis of the finite element model and the medium test specimen

5. Derivation of Target Values in the SAC Study

The SAC loading protocol developed by Krawinkler et al. [3] is used in this study for defining the target values of the loading history. As shown in Fig. 8, several benchmark frame structures (3, 9, and 20 stories) which previously designed in the SAC study, were used as case studies.

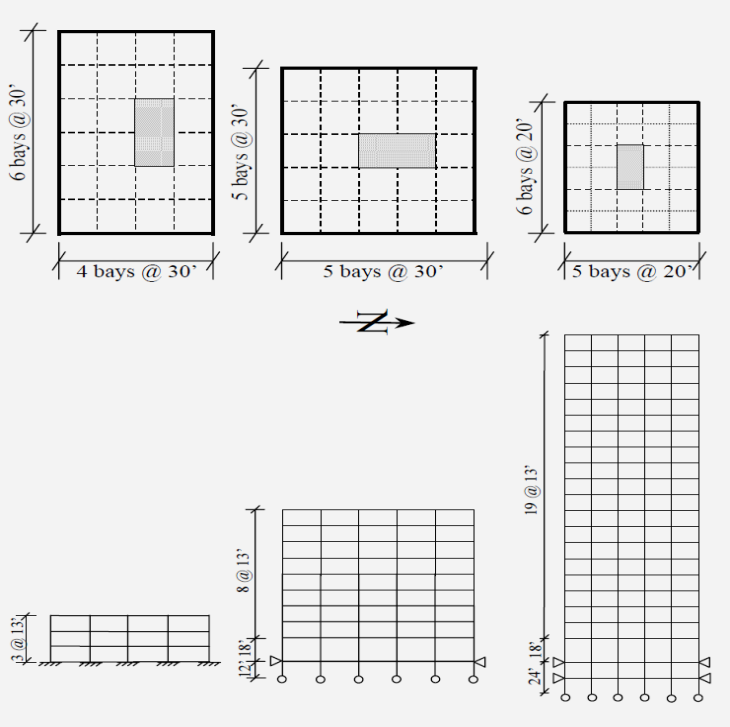

Fig. 8. SAC study moment frames.

Then time history analyses were performed on the frame structures subjected to several sets of ground motion records and the inter-story drift angles versus time were obtained which is shown in Fig. 9. As shown in Fig. 10 maximum deformation range for each level has been obtained under seismic excitation. It was obvious that in 3rd floor of the 3-story structure, deformation range was maximum which made this story critical.

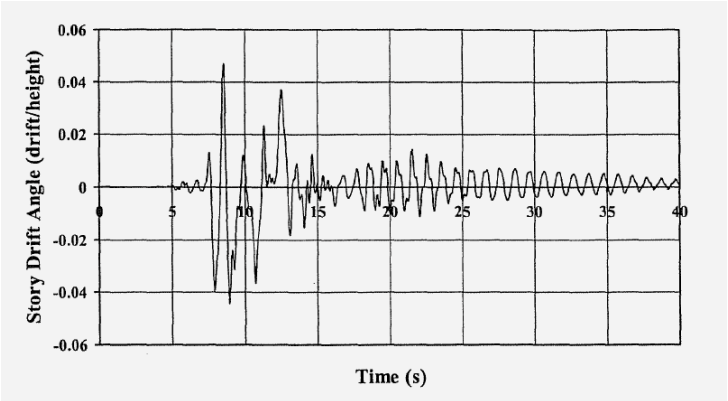

Fig. 9. Time history of story drift angle: story 3 of LA 3 Story [3]

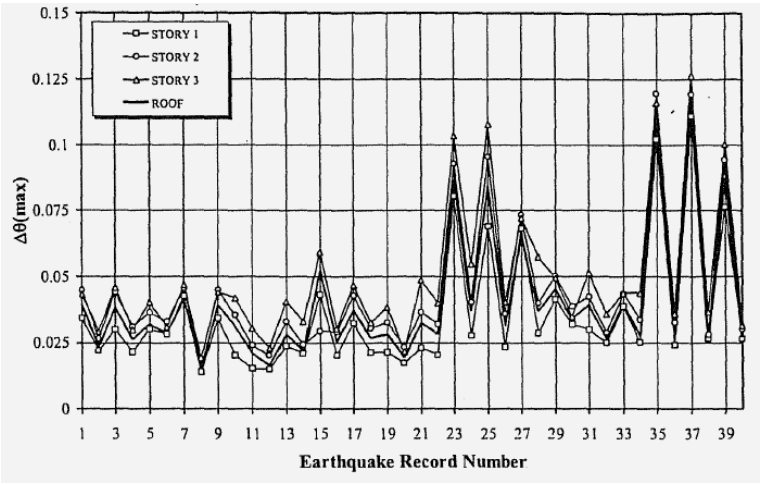

Fig. 10. Maximum story deformation ranges: LA 3 Story.

Then using the rain flow cycle-counting method, the deformation response was converted to a sequence of symmetric cycles. Subsequently, using the statistical distribution and the cumulative distribution functions, the critical story was determined. Critical story is the story in which maximum of demand parameters occurred. Finally, as it is shown in Fig. 11, the target values for producing the loading protocol were chosen from the 50%, 75%, and 90% values of the critical stories. The target values of the loading history are the number of the damage cycles (N_t), the maximum deformation range ($\Delta\theta_{max}$), the maximum deformation amplitude (θ_{max}), and the cumulative deformation range ($\sum\Delta\theta_i$). These target values are presented in Table 2 and total number of cycles is shown in Fig. 11. It has been observed that the 3rd story of the 3-story structure has the maximum total number of cycles. Using 50,70 and 90 percentile values and some criteria which helps protocol to match what likely to be happened in a seismic excitation, target values for SAC loading has been obtained. The number of the damage cycles is the number of the cycles that a connection should be able to endure during an earthquake. Damage cycles have deformation ranges greater than 0.0005 rad. The maximum deformation range is the largest deformation range that a connection should experience a full cycle with it; in order to have its performance verified. The maximum deformation amplitude is one-half of the maximum deformation range. The cumulative deformation range is the sum of the deformation ranges that the connection should endure in order to achieve the desired performance.

Table 2. Target values of the demand parameters of the SAC loading history [2].

N_t	$\Delta\theta_{max}$	θ_{max}	$\sum\Delta\theta_i$
30	0.08	0.04	0.47

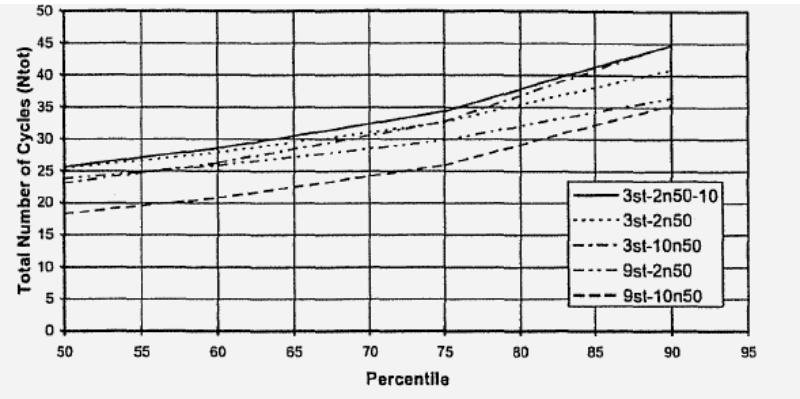

Fig. 11. percentile placing of total number of cycles

6. Demands by the Loading Protocols

As Krawinkler et al. [28-29] stated, all seismic capacity parameters (strength, stiffness, inelastic deformation capacity, and cumulative capacity parameters such as energy dissipation capacity) are expected to deteriorate as the number and amplitude of cycles increase. It is assumed that the onset of deterioration, as well as the rate of deterioration, can be described by a cumulative damage model of the type, as follows:

$$D = C\sum_{i=1}^{N}(\Delta\delta_i)^c$$

Where:

$\Delta\delta I$ = deformation range (total change in deformation) of excursion (or cycle) i

N = number of damaging excursions (or cycles)

C = a structural performance parameter that may depend strongly on the type of component and failure mode

c = structural performance parameter the is usually greater than 1.0.

Table 3 shows the amplitudes and cumulative rotations for the loading protocols investigated in this study. As illustrated, the connections which are analyzed by the SAC basic loading history, need to endure 29 damage cycles in order to reach the maximum target rotation of 0.04 radians, including one complete cycle in this deformation range. At this rotation level, the target cumulative rotation of the loading history must reach 0.59 rad. This loading protocol is developed based on the target values of the study done by Krawinkler et al. [3]. Therefore, this loading protocol has a good consistency with the target values of the study. This loading protocol not only imposes the deformation demand to the connection in the maximum target deformation range of 0.04 rad, but also incorporates the demanded number of the damage cycles in this rotation (29 damage cycles).

In the ATC-24 protocol, the amplitude of the deformation cycles is based on the yield deformation. Because of differences in the yield deformations of the connections, determining the deformation amplitudes in the ATC-24 protocol requires preliminary monotonic loading. In this loading protocol, when the connections experience a complete cycle of the maximum target deformation range (0.04 rad.), the light, medium, and

heavy size connections sustain cumulative rotations of 0.51, 0.52, and 0.52 radians; respectively. As presented in Table 3, the ATC loading protocol fulfills the target cumulative rotation in the cycle in which the maximum deformation range reaches the target value (0.04 radians). This protocol takes into account a conservative value of the cumulative rotation demand (0.01 to 0.08 radians). In this loading protocol, the connections undergo fewer damaging cycles to reach the maximum deformation range, and the loading cycles tend to have larger deformation ranges compared to the SAC and FEMA-461 protocols. Considering the fact that a typical ground motion record has more excitation cycles with smaller deformation ranges than the larger ones, the ATC-24 loading protocol has a weakness in this aspect. Consequently, this loading protocol imposes small number of damaging cycles (13 to 15 cycles less than the target number of the cycles) on the connection.

The connections, which are loaded with FEMA-461, experience 17 damage cycles before reaching the target deformation range. Note that the cycles in the beginning of this protocol have deformation ranges less than 0.005 radians, and are not considered damage cycles. Although these cycles contribute to the cumulative deformation range, they do not impose any damage, while greater values for the capacity parameters were expected. Because the cycles with deformation ranges less than 0.005 radians do not impose any damage to the connection, the numbers of the damage cycles of this loading protocol are less than the target number (13 cycles less). The connections sustained cumulative deformation ranges between 0.56 and 0.58 rad. in the target deformation range of this loading protocol. This is considered to be slightly conservative compared to the target value of this parameter in the FEMA protocol (0.09 to 0.11 radians).

Table 3. Parameters of the loading protocols and their results

SAC loading protocol				
Loading step	Number of cycles in the step	Cumulative number of cycles	Amplitude of inter-story drift angle (rad.)	Cumulative rotation (rad.)
1	6	6	0.00375	0.045
2	6	12	0.005	0.105
3	6	18	0.0075	0.195
4	4	22	0.01	0.275
5	2	24	0.015	0.335
6	2	26	0.02	0.415
7	2	28	0.03	0.535
8	2	30	0.04	0.695

ATC loading protocol							
Loading step	Number of cycles in the step	Amplitude of inter-story drift angle (rad.)			Cumulative rotation (rad.)		
		Light connection	Medium connection	Heavy connection	Light connection	Medium connection	Heavy connection
1	3	0.0054	0.004	0.004	0.0325	0.0241	0.024
2	3	0.008	0.006	0.006	0.0813	0.0604	0.0602
3	3	0.0108	0.008	0.008	0.1464	0.1088	0.1083
4	3	0.021	0.016	0.016	0.2766	0.2055	0.2047
5	3	0.032	0.024	0.024	0.4719	0.3506	0.3492
6	2	0.043	0.032	0.032	0.6455	0.4795	0.4776
7	2	0.054	0.04	0.04	0.8625	0.6407	0.6382

FEMA-461 loading protocol							
Loading step	Number of cycles in the step	Amplitude of inter-story drift angle (rad.)			Cumulative rotation (rad.)		
		Light connection	Medium connection	Heavy connection	Light connection	Medium connection	Heavy connection
1	2	0.0017	0.0009	0.00171	0.00702	0.0036	0.00685
2	2	0.0024	0.0012	0.00239	0.01684	0.00864	0.01645
3	2	0.0034	0.0017	0.00335	0.0306	0.01569	0.02988
4	2	0.00481	0.00246	0.0047	0.04987	0.02557	0.04869
5	2	0.00674	0.00345	0.00658	0.07683	0.0394	0.07502
6	2	0.00941	0.00484	0.00921	0.11459	0.05876	0.11189
7	2	0.01326	0.00672	0.0129	0.16745	0.08587	0.1635
8	2	0.0185	0.00948	0.01806	0.24145	0.12382	0.23575
9	2	0.0259	0.01328	0.02521	0.34505	0.17694	0.33691
10	2	0.03626	0.01859	0.0354	0.49009	0.25132	0.47853
11	2	0.05076	0.02603	0.04956	0.69314	0.35546	0.67679
12	2	0.07106	0.03644	0.06939	0.97742	0.50124	0.95437
13	2	0.09949	0.05102	0.09715	1.37541	0.70534	1.34297

7. Evaluation of the Connections Behavior and Results

In this section, the behavior of the connections has been investigated subjected to different loading protocols. After analyzing the three different connections using the ABAQUS finite element software, results shown in Table 4 are employed in order to explore the performance of the connections. The pertinent parameters that are investigated in this study include the dominant failure mode, strength capacity, deformation capacity at two strength levels, equivalent plastic strain, and dissipated energy. These parameters are investigated in detail in the following sections. Comparisons of cyclic behavior of the connections subjected to study's loading protocols are shown in Figs. 12- 14. Hysteretic behavior of small, medium and large connections impacted by SAC, FEMA and ATC loading represented in figures which is a clear indication of differences of cyclic response of the connections in different loading sequences. With the respect to Figs. 12-14 and table 4, main findings of the study are detailed below.

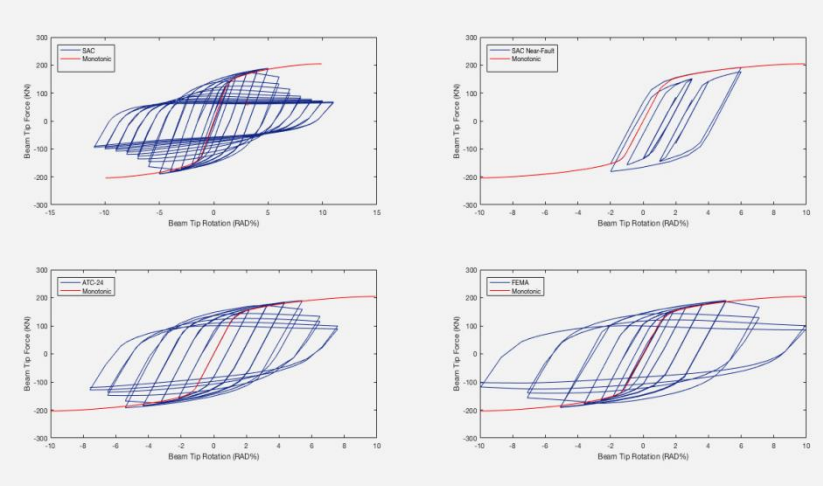

Fig. 12. Cyclic behavior of the small connection with different loading protocols

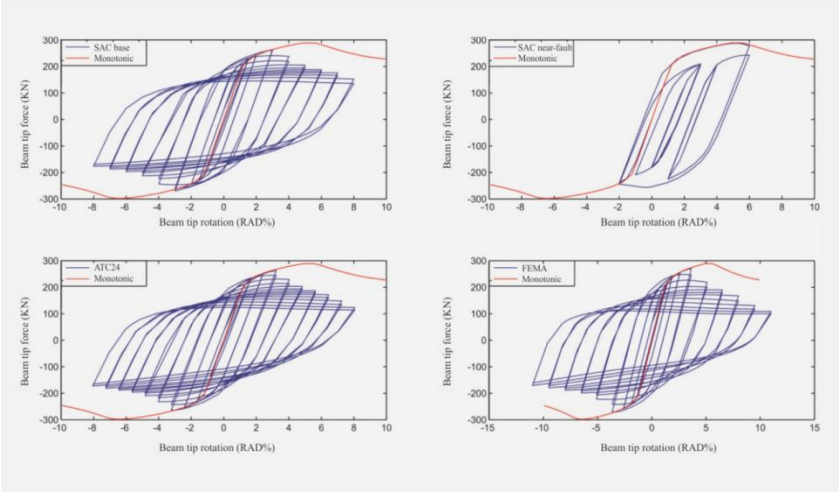

Fig. 13. Cyclic behavior of the medium connection with different loading protocols.

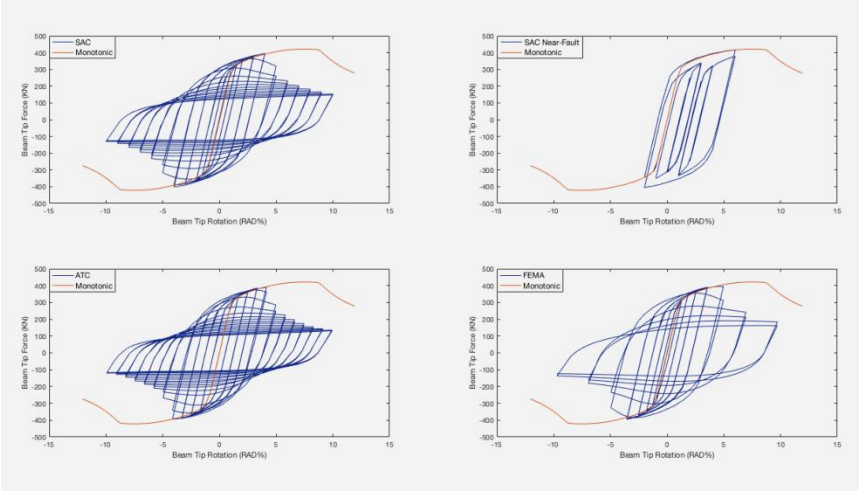

Fig. 14. Cyclic behavior of the large connection with different loading protocols.

Table 4. Behavior and capacity parameters of the connections.

Light connection					
Protocol	Equivalent plastic strain at first rotation equal or greater than 0.04 rad.	Deformation Capacity at 80% of strength (rad.)	Deformation Capacity at 50% of strength (rad.)	Strength capacity (kN.m)	Dissipated energy at first rotation equal or greater than 0.04 rad. (kN.m)
Monotonic	0.03 in the bottom flange	0.154	greater than 0.3	532	-----
ATC	0.48 in the bottom beam flange	0.054	0.075	500	1484.6
SAC	0.375 in the top beam flange	0.060	0.070	495	1209.0
FEMA	0.464 in the top beam flange	0.071	0.100	497	1562.9
SAC near-fault	At the end of loading 0.40 in the bottom weld	Total Deformation Capacity 0.06		499	At the end of loading sequence 784.0
Medium connection					
	Equivalent plastic strain at	Deformation	Deformation	Strength	Dissipated energy at

	first rotation equal or greater than 0.04 rad.	Capacity at 80% of strength (rad.)	Capacity at 50% of strength (rad.)	capacity (kN.m)	first rotation equal or greater than 0.04 rad. (kN.m)
Monotonic	0.11 in the bottom flange	0.094	greater than 0.3	780	-----
ATC	0.6 in the top beam flange	0.04	0.07254	650	2013.6
SAC	0.43 in the top beam flange	0.04	0.09	657	1268.2
FEMA	0.34 in the top beam flange	0.051	0.08	668	2149.4
SAC near-fault	At the end of loading 0.38 in the bottom flange	Total Deformation Capacity 0.06		615	At the end of loading sequence 1212.7
Heavy connection					
	Equivalent plastic strain at first rotation equal or greater than 0.04 rad.	Deformation Capacity at 80% of strength (rad.)	Deformation Capacity at 50% of strength (rad.)	Strength capacity (kN.m)	Dissipated energy at first rotation equal or greater than 0.04 rad. (kN.m)
Monotonic	0.16 in the bottom flange	0.100	0.137	1158.9	-----
ATC	0.73 in the top beam flange	0.042	0.066	1072.2	4110.8
SAC	0.56 in the top beam flange	0.040	0.070	1086.8	2883.9
FEMA	0.72 in the top beam flange	0.049	0.069	1087.9	4236.4
SAC near-fault	At the end of loading 0.44 in the bottom weld	Total Deformation Capacity 0.06		1006.7	At the end of loading sequence 2282.0

7.1. The Dominant Failure Mode

In order to investigate the dominant mode of failure, equivalent plastic strain (PEEQ) is used as the determinant index. It is required to monitor its rate of increase as well as controlling its location in the connections. The maximum values for equivalent plastic strain per connections and its position is presented in Table 4. In most connections under different loading conditions, values of PEEQ had the maximum values at the upper and lower flange and this increase in strain reflects the beam flange local buckling. Fig. 15 displays a typical contour of the equivalent plastic strain for the medium connection at the instant of failure. As displayed the concentration of the PEEQ is mostly around the beam flanges near to the connection ranging 0.033 to 0.056 with the maximum value of 0.056. Light and heavy connections subjected to SAC near-fault loading protocol display different behavior compared to the medium connection. As specified in Table 4, maximum values of PEEQ in these two connections extended into the bottom welds, which is not desirable, and lead to rapid strength deterioration. von-Mises stress contours at the instant of failure in the medium connection subjected to SAC loading is displayed in Fig. 16. Again, the concentration of the maximum value of the von mises stress is near the vicinity of the connection. It must be noted that the instant of the failure is considered the instant when twenty percent strength loss is experienced in the connection. As illustrated in the Figure, it is clear that von mises stress values in weld are lower than steel ultimate stress; which were seen in all cases.

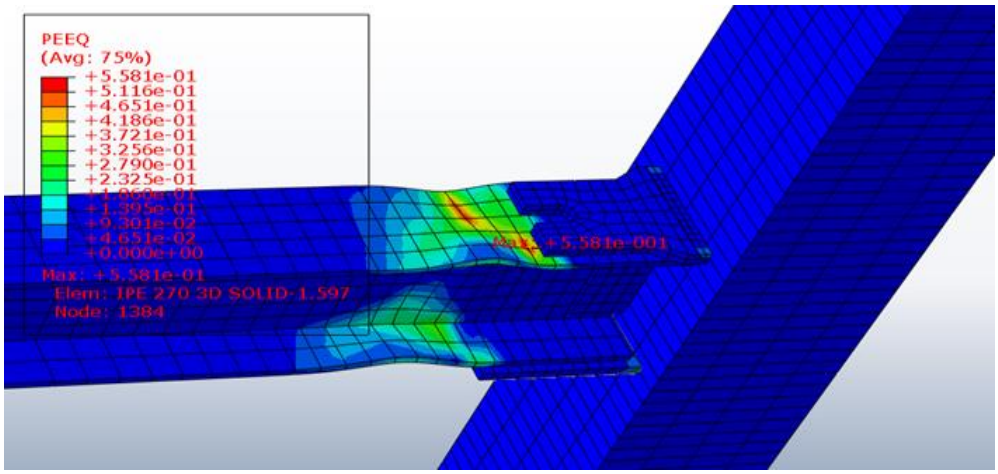

Fig. 15. Contour of the equivalent plastic strain at the instant of failure of the medium connection.

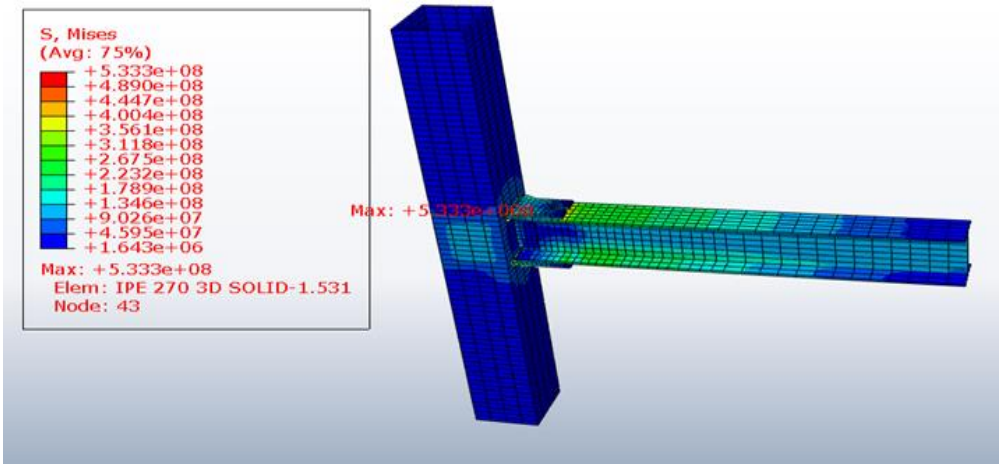

Fig. 16. Contour of the von-mises stress at the instant of failure of the medium connection.

7.2. Strength Capacity

When subjected to monotonic loading, all connections reached the highest level of its strength. Connections under far field cyclic loading show almost the same level of strength. According to Table 4 in light connection, the highest level of strength under ATC loading is 500 kN.m and minimum level of it under SAC loading is 495 kN.m. In the medium connection, the highest level of strength under FEMA loading is 668 kN.m. The lowest level of strength under ATC loading is 650 kN.m. As shown in Table 4, in heavy connection, the highest and lowest level of strength under FEMA and ATC loading is 1088 and 1072 kN.m; respectively. According to this result, it was found that the type of cyclic loading sequence has no significant effect on strength capacity of three connections. Connections under SAC near field loading demonstrated behavior very similar to monotonic loading behavior. Connections strength under this loading is shown in Table 4. A similar behavior of Connections under this loading with near field SAC is while the connection is pushed.

7.3. Deformation Capacity

Deformation capacity of connections in two levels of strength loss is investigated. First level of deformation capacity of connections is in its twenty percent strength

loss and the second level for near collapse behavior is its fifty percent strength loss. All the Connections are analyzed on these two levels strength loss under different loading and the results are shown in Table 4. The details of the results observed for the different level of strength loss is as follows:

7.3.1 Twenty Percent Level of Strength Loss

According to Table 4, in the light connection, deformation capacity values under FEMA and ATC loading has the highest and lowest level of 0.071 and 0.054 radians; respectively. Also in medium connection, maximum deformation capacity under FEMA loading is 0.051 radians; while it is 0.040 radians under SAC and ATC which t is lower than values obtained by FEMA loading. As shown in Table 4, maximum strength capacity of heavy connection under FEMA loading is 0.490 radians; and the minimum capacity of connection deformation under SAC loading is 0.040 radians. In this level, strength loss of three connection reach to maximum strength capacity under FEMA loading. Connections deformation capacity under SAC and ATC loading has similar behavior and connections strength capacity under these loading is lower than FEMA loading. This difference in deformation capacity of light, medium and heavy connections is 31.0, 27.5 and 22.5 percent; respectively.

7.3.2. Fifty Percent Level of Strength Loss

In the fifty percent level of strength loss in the light connection, maximum deformation capacity under FEMA loading is 0.10 radians. Minimum deformation capacity under FEMA loading is 0.10 radians. Minimum deformation capacity of connection as shown in Table 4 under SAC loading is 0.07 radians. Maximum deformation capacity of medium connection in this level of strength loss under SAC loading is 0.09 radians and its minimum under ATC is 0.072 radians. In heavy connection maximum and minimum values under FEMA and SAC is 0.07 radians and ATC is 0.066 radians. In this strength loss, difference in strength capacity of connection between deformation capacities of connections under different loads is significant. This difference for heavy, medium and light connections is 6, 24 and 30 percent. The difference between the values of deformation capacity for per connection under cyclic loading shows high sensitivity of this parameter to loading deformation sequence. As the damage is cumulative and each connection has memory of losses incurred from the beginning of loading cycles. All connections subjected to monotonic loading reach its maximum deformation capacity, which was predictable. All three connections under near field SAC loading during the deformation sequence and their performance was acceptable. In this loading due to the nature of the deformation sequence of connections, the performance of connections for rotation reaches to 0.06 radians.

7.4. Equivalent Plastic Strain

After the first cycle of the loading sequence, at deformation of 0.04 radians, equivalent plastic strain was evaluated for the connections. In Table 4, the maximum equivalent plastic strain and its location is indicated. It was found that the sequence of loading has a large impact on equivalent plastic strain of connections. After the first cycle of 0.04 radians, the maximum of PEEQ for light connection due to ATC loading is 0.48. In the medium and heavy connections under ATC loading, the maximum value of PEEQ are 0.60 and 0.73; respectively. In all cases, the maximum equivalent plastic strain

was observed in the upper flange of beam. PEEQ is significantly affected by loading protocol and therefore under different loading protocol considerable differences are displayed. As shown in Table 4, this difference for light, medium and heavy connection is 28, 76 and 30 percent; respectively. In the all connections, the maximum equivalent plastic strain was found in the ATC loading protocol. Connections under FEMA loading and SAC loading had the minimum values of equivalent plastic strain. Reason of higher cumulative strain on connections under ATC and FEMA loading is the existence of cycles with higher damage amplitudes in comparison with the SAC loading protocol. Most cumulative rotation by ATC and FEMA protocols is attained by cycles with larger amplitude that lead to more damage on the performance of the connection. As expected, connections under monotonic loading have the least PEEQ strain, which is mainly due to its nature of not being cyclic. Values of PEEQ strain of connections under near field SAC loading are measured at the end of loading as shown in Table 4; which indicate that values of equivalent plastic strain in all connections subjected to near fault SAC loading are well below the same connections subjected to cyclic loading. This is mainly due to higher number of cycles of loading compare to near fault SAC loading, which they impose higher demands on the connection in comparison with demands imposed by near fault loading on connections.

7.5. The Dissipated Energy

Dissipated energy of connection after completion of the last cycle equal to 0.04 radians or greater is investigated. As shown in Table 4, light connection under FEMA loading has most dissipation of energy 1562.9 kN.m. With slight difference about 5%, connection under ATC loading protocol has less dissipated energy than FEMA loading. Light connection under SAC loading protocol has less dissipated energy than the other two loading protocol being around 29%. Similarly, at medium and heavy connection, under FEMA and ATC loading protocol the energy dissipation of the connection was higher than the other protocol. All three connections under SAC loading have the least amount of dissipated energy among all the loadings. This is mainly because the SAC loading has cycles with small deformation amplitude range that forces the connection to the nonlinear range in later phase. In the ATC and FEMA protocols, in order to satisfy the conditions of qualification, connections need to withstand greater deformation range, which would impose greater demands on the connection. In light connection, ATC need to withstand range of 0.054 radians and FEMA need to withstand range of 0.051 radians. For the medium and light connection under FEMA protocol demand for rotation is 0.051 and 0.0496; respectively. As the less number of cycles for near field SAC protocol, the dissipated energy at the end of the cycles as it shown in Table 4 has smaller quantities.

8. The Proposed Loading Protocol

A loading protocol is developed in order to match the loading history of the steel moment connections as close as possible to the demands imposed on steel moment resisting frames' connections in an earthquake event. The proposed loading protocol subjected to connections and results compared to those of other cyclic loadings. The new protocol illustrated the fact that two nearly identical sequences which only differ in the size of some cycles and their numbers

can be effective on the behavior of connections and capacity parameters of connections.

Target values for development of SAC loading protocol for steel moment frame structures' connections are presented in Table 2, which includes the number of damage cycles, range of deformation. The cumulative deformation presented in Table 2 attained following the procedure described in section 5. In this study, the target values from the SAC study adopted in order to develop a loading protocol that can simply be used by researchers and represent the local demands on connections in a seismic event. In the development of this loading protocol, special attention is given to the following points. First, in a real seismic event, probability of occurrence of a cycle with a large range of deformation is very little compared to the probability of occurrence of cycles with a small range of deformation. Therefore, in the development of the loading protocol, in each step of increase in the loading range, the number of the cycles in that step is decreased. In this manner, cumulative deformation demands of proposed loading protocol come mostly from cycles with small deformation ranges and gradually with an increase in deformation ranges and number of cycles are decreased. Consequently, the number of the cycles having smaller deformation range is greater than the number of the cycles with larger deformation range. Secondly, in order to prevent the low cycle fatigue conditions, the cycles at the beginning of the loading protocol have deformation ranges smaller than the yield deformation range. Moreover, proposed loading protocol avoids using cycles with deformation range smaller than 0.005 radians. Therefore, all cycles having deformation ranges greater than 0.005 radians in this loading protocol are damaging cycles. The third and the most important point taken into account in development of this loading protocol are reaching the chosen target values. The connection has to meet the demand imposed by this loading protocol. Finally, in order to reach the aforementioned goals, the authors develop the proposed loading protocol as it shown in Fig. 17.

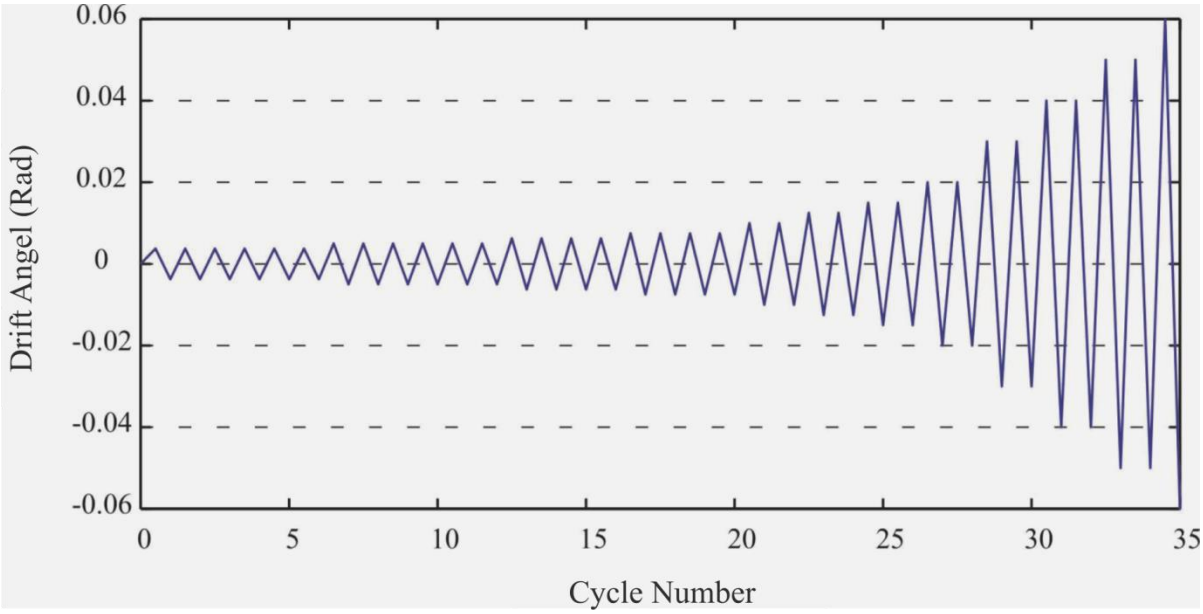

Fig. 17. The proposed loading protocol

In the proposed loading protocol, the target maximum deformation range is set at 0.040 radians. According to Table 5, the proposed loading protocol reaches the target deformation range in the 10^{th} step, after 30 load cycles; and the connection sustains a cumulative deformation of 0.590 radians. Because the cumulative deformation in the 30^{th} loading cycle is 0.120 radians greater than the target value of this parameter (0.470 radians), the proposed loading protocol imposes a quite conservative cumulative deformation on the connection. The deformation range of 0.0075 radians is chosen for the smallest cycles, which is greater than 0.005 radians. Consequently, in the proposed protocol, only damaging cycles are imposed on the connection, and damage is imposed on connection in every cycle.

All three connections subjected to the proposed loading are analyzed in finite element software and moment rotation curve obtained; as illustrated in Fig. 18. As presented in Table 6, connections behavior and their parameters under this loading are quite different in comparison with other loadings. Deformation capacity of connections in twenty percent loss, under proposed loading is different with respect to the SAC protocol that was used to as a basis of the production of the proposed protocol. Light connection under proposed and SAC loading reached to 0.060 radians of rotation. However, medium and heavy connection rotation under proposed loading reached 0.05 radians rotation while under SAC loading, they reached 0.04 radians. In fifty percent loss level, the rotation in light connection under proposed loading is greater than 0.09 radians and under SAC loading is 0.07 radians. Strength capacity of connections under proposed loading is slightly more than other cyclic loading protocols. According to the results presented in Tables 4 and 6, this difference is negligible in light connection but in medium connection under proposed loading, strength capacity is 720 kN.m and it is 63 kN.m more than SAC loading and it is 52 kN.m more than FEMA loading. In heavy connection under proposed loading, strength capacity is 23 kN.m more than SAC and FEMA loading. The equivalent plastic strain in heavy and light connection under SAC loading is greater than proposed loading. Also in heavy and light connection under proposed loading, equivalent plastic strain in welds is increased and reached its maximum level which indicates the inadequacy of the connections. On the contrary, in those two connections subjected to SAC protocol, maximum of equivalent plastic strain occurred in beam's flanges. Results in Tables 4 and 6 indicate that dissipated energy of connections under proposed loading is significantly less than other cyclic loading protocols. In light connection, this parameter under proposed loading is 77.5 kN.m and under SAC loading is 1209 kN.m. In a similar way for medium and heavy connection, dissipated energy under proposed loading is 1134.4 kN.m and 2439.7 kN.m and it is lower than connections subjected to SAC loading with 1268.2 kN.m and 2883.9 kN.m. Proposed loading protocol has less cycle with larger amplitudes than SAC loading and most range of deformation is provided by small amplitude cycles. This causes less demands on connections that makes larger rotation, more strength capacity and less dissipated energy demand than connections under SAC loading.

Table 5. Number of cycles and deformation amplitude of the loading steps of the developed loading protocol.

Loading step	Maximum deformation amplitude	Number of the cycles in the step
1	0.00375	6
2	0.005	6
3	0.00625	4
4	0.0075	4
5	0.01	2
6	0.0125	2
7	0.015	2
8	0.02	2
9	0.03	1
10	0.04	1
11	0.05	1
12	0.06	1
13	0.07	1
14	0.08	1

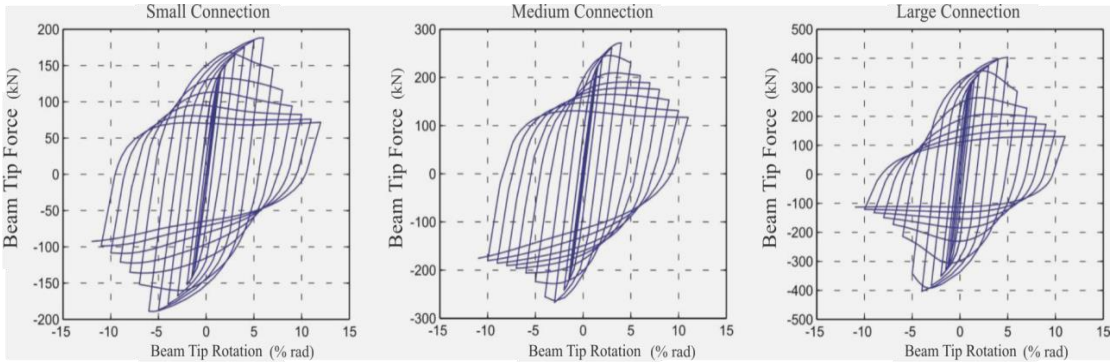

Fig. 18. Behavior of the connections subjected to the proposed loading protocol.

Table 6. Behavior and the capacity of the connection subjected to the proposed loading.

Equivalent plastic strain at first rotation equal or greater than 0.040 radians	Deformation Capacity at 80% of strength (radians)	Deformation Capacity at 50% of strength (rad.)	Strength capacity (kN.m)	Dissipated energy at first rotation equal or greater than 0.040 radians (kN.m)
Light connection				
0.036 in the bottom weld	0.06	0.09	501	775.6
Medium connection				
0.45 in the bottom weld	0.05	0.09	720	1134.4
Heavy connection				
0.48 in the top beam flange	0.05	0.07	1109	2439.7

9. Conclusion

This study revealed that the imposed loading history has a great effect on the performance and capacity parameters of the connections, and choosing a suitable test schedule better helps to understand the behavior of a connection in the seismic excitations.

The ATC loading protocol is mainly composed of large amplitude cycles. Therefore, the demands imposed on the connection by this loading protocol are unrealistic (much less number of damage cycles). The FEMA protocol had the number of the damaging cycles less than the target number.

Type of loading protocol demonstrated to have not great effect on dominant failure mode. In addition, strength capacity of connections demonstrated low sensitivity to loading protocols. On the other hand, dissipated energy, equivalent plastic strain, and deformation capacity in level of acceptance and near collapse can be very sensitive to loading protocol sequence. Monotonic loading having a non-cyclic nature and due to small demand, which it imposes to connection has a different behavior than cyclic loading. Connections subjected to monotonic loading displayed larger strength and deformation capacity. In addition, less cumulative deformation demands of monotonic loading compared to cyclic loadings, connections subjected to monotonic loading resulted in smaller equivalent plastic strain compared to same connection subjected to cyclic loadings. All connections analyzed with SAC near-fault protocol easily reached the 6% target ultimate rotation in either positive or negative direction; and it was revealed that the connection can further experience higher levels of rotation even beyond enduring the entire cycles of this protocol. All the connections loaded with cyclic or monotonic loading experience a failure mode of local buckling in the beam flange.

A loading protocol is developed and proposed based on the condition of meeting all the target demand values resulted from nonlinear two-dimensional analysis of the SAC frames subjected to a set of ground motions. Comparing the proposed loading with SAC loading protocol, it is clear that the effect of range amplitude and loading steps on connection behavior is very significant. Connections subjected to proposed loading reached higher deformation and strength capacity. In addition, those connections needed to dissipate less energy compared to those connections subjected to SAC loading. This difference on energy dissipation came from higher demands which SAC loading protocol imposes compared to proposed loading. Proposed loading protocol has more small cycles, which makes less demand on connections than SAC loading. In light and medium connection subjected to the proposed loading, it has been observed that equivalent plastic strain in welds have higher values which might lead to rapid strength loss of the connections.

The authors suggest further numerical as well as experimental studies on the subject in order to produce series of loading protocol based on the seismic zone and structural period. A comprehensive study with respect to regional seismic event and conventional frames which are currently in use in Iran has to be conducted in order to develop series of loading protocols for steel moment resisting frame connection.

REFERENCES

[1] ATC-24 (1994) Guidelines for Cyclic Seismic Testing of Components of Steel Structures for Buildings, Applied Technology Council, Redwood City, CA., USA.

[2] Clark, P., Frank, K., Krawinkler, H., and Shaw, R. (1997) "Protocol for fabrication, inspection, testing, and documentation of beam-column connection tests and other experimental specimens," SAC Steel Project Background Document. October, Report No. SAC/BD-97/02.

[3] Krawinkler, H., Gupta, A., Ibarra, L., Medina, R., and Luco, N. [2000] "Loading histories for seismic performance testing of SMRF components and assemblies," SAC Steel Project Background Document. August, Report No. SAC/BD-00/10.

[4] Federal Emergency Management Agency (2007) Interim Testing Protocols for Determining the Seismic Performance Characteristics of Structural and Nonstructural Components, FEMA Report 461, Washington, USA.

[5] Behr, R.A. and Belarbi, A. (1996) "Seismic test methods for architectural glazing systems," Earthquake Spectra, 12(1), 129–143.

[6] Krawinkler, H., Parisi, F., Ibarra, L., Ayoub, A., and Medina, R. (2001) Final Report, "Development of a testing protocol for wood frame structures," CUREE-Caltech Wood frame Project Report, Stanford University, CA, USA.

[7] EN-12512 (2001) Timber Structures-Test methods. "Cyclic testing of joints made with mechanical fasteners," European Committee for Standardization, Brussels.

[8] Retamales R., Mosqueda G., Filiatrault A. and Reinhorn A. (2011) "Testing protocol for experimental seismic qualification of distributed non-structural systems," Earthquake Spectra, 27(3), 835–856.

[9] Hutchinson T., Zhang J. and Charles E. (2011) "Development of a drift protocol for seismic performance evaluation considering a damage index concept," Earthquake Spectra, 27(4), 1049- 1076.

[10] Yu, Q. S., Gilton, C. S. and Uang, C.M. (1999) "Cyclic response of RBS moment connections: loading sequence and lateral bracing effects," Report No. SSRP 99-13, University of California at San Diego, CA., USA.

[11] Gatto, K. S. and Uang, C.M. (2003) "Effects of loading protocol on wood frame shear wall response," Journal of Structural Engineering, 129(10), 1384-1393.

[12] ISO, (1998) Timber Structures Joints Made with Mechanical Fasteners Quasi-Static Reversed-Cyclic Test Method, ISO/TC 165 WD 16670, Secretariat, Standards Council of Canada.

[13] Porter, M.L. (1987) "Sequential phased displacement (SPD) procedure for TCCMAR testing" Proc. of 3rd Meeting of the Joint Technical Coordinating Committee on Masonry Research, US-Japan Coordinated Research Program.

[14] Okazaki, T., Arce, G., Ryu, H.C., and Engelhardt, M. D. (2005) "Experimental study of local buckling, over strength and failure of links in EBFs," Journal of Structural Engineering, 131(10), 1526–1535.

[15] AISC/ANSI 341-05 (2005) Seismic Provisions for Structural Steel Buildings. American Institute of Steel Construction, Chicago, Il., USA.

[16] Richards, P. and Uang, C.M. (2006) "Testing protocol for short links in eccentrically braced frames," Journal of Structural Engineering, American Society of Civil Engineer, 132(8), 1183- 1191.

[17] Shafei, B. and Zareian, F. (2008) "Development of a quasi-static loading protocol for displacement-sensitive nonstructural building components," In Proc. of the 14th World Conference on Earthquake Engineering, Beijing, China.

[18] Jiao, Y., Kishiki, S. and Yamada, S. (2012) "Loading protocols employed in evaluation of seismic behavior of steel beams in weak-beam moment frames" In Proceeding of 15th World Conference on Earthquake Engineering, Lisbon, Portugal.

[19] Bazaez, R., & Dusicka, P. (2014) "Development of Cyclic Loading Protocol for Bridge Columns Considering Subduction Zone Mega Earthquakes", In Proceeding of the 10th National Conference in Earthquake Engineering, EERI, Anchorage, Alaska.

[20] Mergos P, Beyer K. (2014) "Loading protocols for regions of low to moderate seismicity in Europe," Bulletin of Earthquake Engineering, 12(6), 2507-2530.

[21] Mergos, P., & Beyer, K. (2015). Loading protocols for structures designed for different behavior factors. In Proceedings of the SECED 2015 Conference (No. EPFL-CONF-217006).

[22] ISO-21581 (2010) Timber Structures-Static and cyclic lateral load test methods for shear walls, International Standards Organization, Geneva, Switzerland.

Japan Iron and Steel Federation [2002] Testing methods of the evaluation of structural performance for the steel structures, Japan.

[23] SaneeiNia, Z., Mazroi, A., and Ghassemieh, M. (2014) "Cyclic performance of flange-plate connection to box column with finger shaped plate", Journal of Constructional Steel Research, 101, 207-223.

[24] Saneei Nia, Z., Ghassemieh, M. and Mazroi, A. (2014) "Panel zone evaluation of direct connection to box column subjected to bidirectional loading", Structure Design of Tall and Special Buildings, 23, 833-853.

[25] Iranian national building code (2005) Design and Construction of Steel Structures, Tehran, Iran.

[26] Iranian Standard 2800 (2010]) Formulation of Building Design Codes for Earthquakes, Building and house research center, Tehran, Iran.

[27] HKS. ABAQUS user's manual version 6.4. (2003]) Hibbit, Karlsson & Sorensen Inc: 1080 Main Street, Pawtucket, RI 02860, USA.

[28] Krawinkler, H. and Zohrei, M. (1983) "Cumulative damage in steel structures subjected to earthquake ground motions," Journal on Computers and Structures, 16, 531-541.

[29] Krawinkler, H., Zohrei, M., Lashkari, I.M., Cofie, N., and Hadidi T.H., (1983) "Recommendations for experimental studies on the seismic behavior of steel components and materials," John A. Blume Earthquake Engineering, Center, Report No. 61, Department of Civil Engineering, Stanford University, USA.